DOI: 10.2478/fas-2022-0003
FATIGUE OF AIRCRAFT STRUCTURES
Volume 2022: Issue 14, pp. 18-28

THE INFLUENCE OF MATERIAL CONFIGURATION OF FIBRE-METAL LAMINATES WITH ALUMINA CORE ON FLEXURAL STRENGTH

Mariusz Frankiewicz[1*], Michał Karoluk[1], Robert Dziedzic[1],
Tristan Timmel[2], Peter Scholz[3]
[1]Faculty of Mechanical Engineering, Wroclaw University of Science and Technology,
Lukasiewicza 5, 50-371 Wroclaw, Poland
[2]Institute of Lightweight Structures and Polymer Technology, Technische Universität
Chemnitz, Reichenhainer Str. 31-33, 09126 Chemnitz, Germany
[3]Fraunhofer Institute for Machine Tools and Forming Technology IWU,
Reichenhainer Str. 88, 09126 Chemnitz, Germany

mariusz.frankiewicz@pwr.edu.pl

Abstract

Fibre metal laminates (FMLs) consisting of layers made of PA6 polyamide prepregs reinforced with glass and carbon fibres and an aluminium alloy core are the new variant of the other types used by aerospace FML materials such as GLARE or CARALL. By using a thermoplastic matrix, they can be shaped by stamping processes, which allows for a more efficient production process than classical laminating methods such as vacuum bagging. In addition to the improved impact energy absorption efficiency, the metallic core can be utilised to effectively bond the composite part to adjacent metallic structures. This article presents the influence of the material configuration of fibre-metal laminates consisting of continuous fibre-reinforced thermoplastic outer layers integrated with a layer of metallic aluminium alloy inserts—a number of layers, type and direction of reinforcing fibres—on the static and fatigue flexural properties. In this study, eight laminate configurations were prepared using a one-step variothermal consolidation process. The results showed that in the three-point flexural fatigue test, the samples exceeded 10^6 cycles at stresses <30% of the static bending strength. Laminates with predominantly longitudinally reinforced layers showed the highest fatigue strength among the FML samples analysed. The type of reinforcing fibres and the number of layers were less affected on the analysed mechanical properties.

Keywords: fibre-metal laminates, flexural strength, fatigue, composite materials
Article category:

Introduction

Fibre metal laminates (FMLs) (Gunnink, Vlot, Vries, & van der Hoeven, 2002) are materials combining fibre-reinforced polymer (FRP) matrix composite with metal sheets. One of the first FMLs was developed for aerospace structures in the 1980s at the Delft University of Technology (Gunnink et al., 2002). Different types of FML materials, differing in types of reinforced fibres, were developed: GLARE using glass fibres (GF), CARALL reinforced by carbon fibres (CF) or ARALL with aramid fibres (Alderliesten, 2017). One of the first applications of FML was the fuselage components of the Fokker F27 aircraft using ARALL structures, one of the latest is the A380, whose aircraft frame is made in 3% of GLARE (Giasin & Ayvar-Soberanis, 2017) and 22% of the fuselage components produced with glass FRPs (GFRPs) and carbon FRPs (CFRPs). The main purpose of FMLs was to increase the fatigue resistance of components (Giasin & Ayvar-Soberanis, 2017) combined with the light-weight properties (Gunnink et al., 2002). Additional benefits related to these materials are increased damage tolerance and high impact strength (Bellini, Di Cocco, Iacoviello, & Sorrentino, 2020). The matrix of commercially used FMLs (GLARE and ARALL) mainly uses thermosetting materials such as epoxy resins (Zopp et al., 2019). However, they are associated with limitations in component manufacturing such as high costs, low efficiency of manufacturing processes (vacuum bagging) and limited recycling (Ding, Wang, Luo, & Li, 2021). Recently, new developments have been developed in FMLs using thermoplastic matrices, which allow for more efficient thermoforming processes, increased recyclability and greater impact loading strength (Zopp et al., 2019). However, these materials are rarely described, and few research results have been published on the static and fatigue performance of the FML thermoplastic matrix (Zopp et al., 2019).

Since one of the most common causes of FML failure is flexural stress when subjected to bending loads of frame parts (Bellini et al., 2020), and the analyses of bending failures help to assess the quality of the material (Li et al. 2018), this article presents the results of flexural static and fatigue analyses performed on FMLs developed under the Cornet 22/InverTec project.

Materials and Methods/Experimental Procedure

The FMLs used for the tests were made from a 1 mm thick sheet of 6061 T4 aluminium alloy as a core and FRP prepregs (Ticona Celstran), containing 60% by weight fibres in the PA6 matrix: 1.15 mm thick CFRP and 0.29 mm thick GFRP plies. Before consolidation of plies of the laminate, the surface of the 6061 alloy core was grit-blasted to increase adhesion to the FRP layers. The samples for the three-point bend test were prepared in four material configurations differing by the number of GFRP and CFRP plies and two variants differing by fibre arrangement. The configurations and variants of the FMLs are shown in Table 1.

Table 1. Configuration of the analysed series of FMLs

Series	Configuration of FRP laminate layers	Laminate code
S1_0	3x PA6-GF60	$[0^G/90^G/0^G/Alu]_S$
S1_90	3x PA6-GF60	$[90^G/0^G/90^G/Alu]_S$
S2_0	3x PA6-GF60	$[0^G{}_3/Alu]_S$
S2_90	3x PA6-GF60	$[90^G{}_3/Alu]_S$
S3_0	1x PA6-CF60/4x PA6-GF60	$[0^C/0^G{}_4/Alu]_S$
S3_90	1x PA6-CF60/4x PA6-GF60	$[90^C/90^G{}_4/Alu]_S$
S4_0	1x PA6-CF60/4x PA6-GF60	$[0^C/90^G/0^G/90^G/0^G/Alu]_S$
S4_90	1x PA6-CF60/4x PA6-GF60	$[90^C/0^G/90^G/0^G/90^G/Alu]_S$

FMLs, fibre metal laminates; FRP, fibre-reinforced polymer.

The 400 mm × 300 mm plates of the FMLs were made by variothermal consolidation according to the process diagram shown in Figure 1 and the parameters in Table 2. The specimens were cut off from the FML plates according to the ATSM standards guiding the tests.

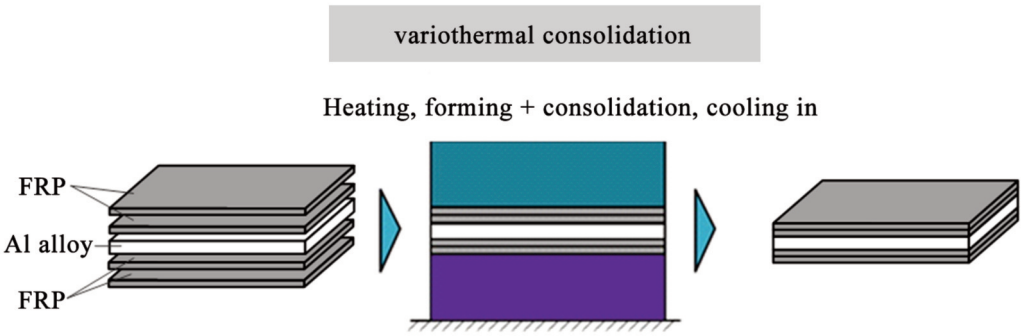

Figure 1. Diagram of the process of forming an analysed FML (InverTec laminate). FMLs, fibre metal laminates; FRP, fibre-reinforced polymer.

Table 2. Parameters of variothermal consolidation of InverTec inverted laminate sheets

	Pressure (bar)	Temperature (°C)	Time (min)
Heating and plasticising of polymer matrix	20	260	6.5
Consolidation of the FRP composite	30	260	3.5
Cooling phase and solidification of the polymer melt	30	601	6.5

FRP, fibre-reinforced polymer.

The mechanical properties of the specimens were determined in the course of the three-point static and fatigue bend tests. Both static and fatigue three-point bend tests were performed as per ASTM D7264/D7264M−15 at room temperature on a servo hydraulic fatigue machine equipped with a three-point bending test device. The dimensions of the samples for the static three-point bend test were 120 mm × 12 mm × 2.8 mm and 140 mm × 20 mm × 2.8 mm for fatigue tests.

During the tests, the specimens were placed on two supports formed by two parallel rolls (Figure 2), positioned centrally, at an equal distance between the support rolls.

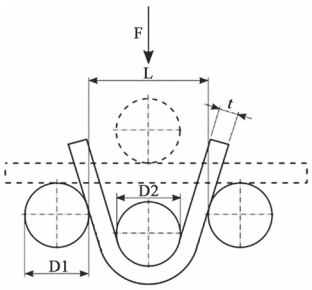

Figure 2. Scheme of the three-point bend test.

Static three-point bend test

The static three-point bend tests were performed in such a manner that a gradually and continuously increasing load was exerted in the middle of the specimen's span by the upper anvil perpendicular to the surface of the specimen.

The tests were performed with the following parameters:

- spacing between the supports was L = 80 mm,
- upper anvil diameter was D2 = 10 mm,
- support diameter was D1 = 5 mm
- bending speed was 5 mm/min

The tests were carried out until the moment of registering a significant and sudden decrease in the value of the bending force, caused by the specimen fracture.

Fatigue three-point bend test

The fatigue three-point bend tests were performed on hybrid laminate series S1_0 and S2_0, as presented in Table 1, in such a manner that a sine-shaped deflection with an unsymmetric load ratio was exerted in the middle of the specimen's span by the upper anvil perpendicular to the surface of the specimen. The hybrid laminate specimens were investigated without any initial notches or precracks.

The tests were performed with the following parameters:

- spacing between the supports was L = 117 mm,
- upper anvil diameter was D2 = 10 mm,
- support diameter was D1 = 5 mm
- frequency: 5Hz

The tests were conducted until run out when specimens reach a fatigue limit of 10^6 cycles or the moment of registering a significant, sudden decrease in the value of the bending force, caused by the specimen fracture.

Results

The results of static three-point bending tests are shown in Figures 3 and 4. The graph in Figure 3 shows the bending curves of bend tests for five samples of each series. The analysis of elastic strains in three-point bending tests indicates that the differences in particular series can be observed regarding the fibre orientation, and samples S2_0 and S3_0 with unidirectional reinforced fibres oriented perpendicular to the bending axis show a higher value of flexural stress because reinforced fibres take part in load transfer.

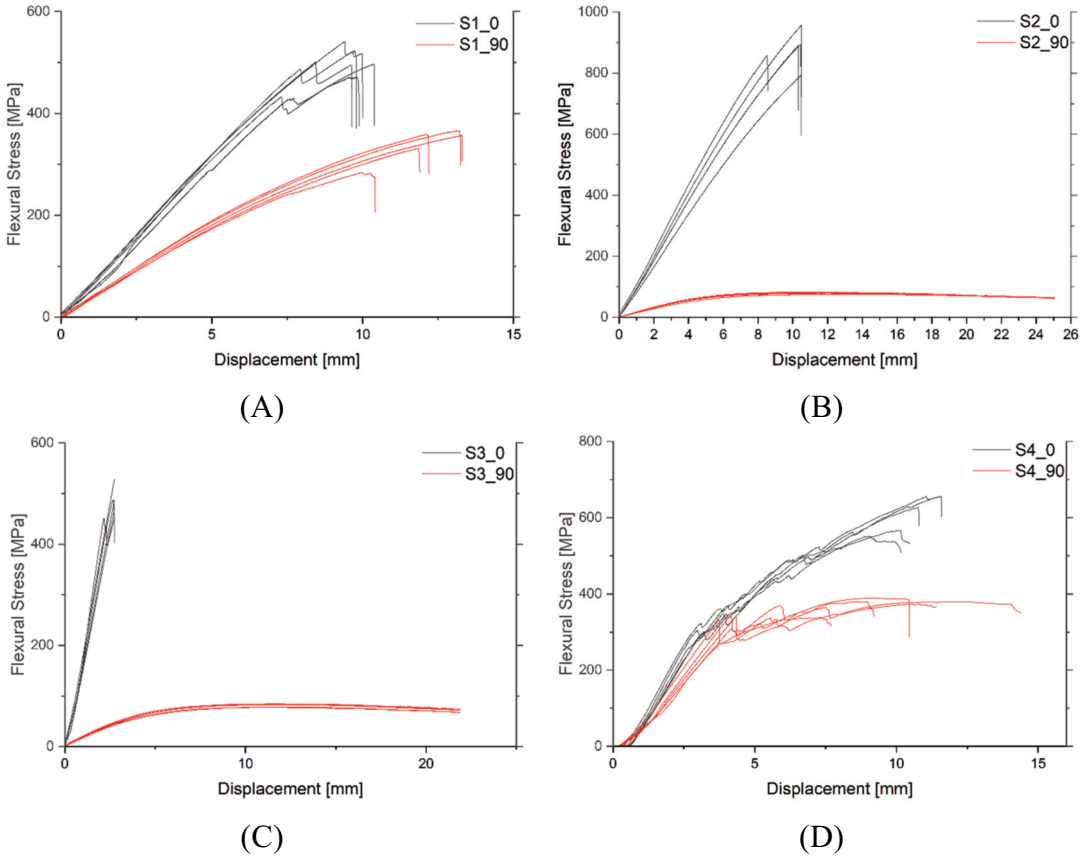

Figure 3. Results of the static three-point bend tests presented by flexural stress vs. displacement graphs, for specimens' series: S1 (A), S2 (B), S3 (C) and S4 (D).

It is clear that there are significant differences between the flexural strengths of variants 0 and 90 for S2 and S3 series (Figures 3B and 3C). Higher values of flexural stress were observed for the laminate series S2_0 reinforced by GF oriented only perpendicular to the bending axis. The maximum value of the flexural stress (878 42 MPa) was observed for the unidirectional laminate series S2_0 reinforced with GF oriented perpendicular to the bending axis. The minimum value of the flexural stress (80 2 MPa) was observed for the laminate series S2_90 with GF oriented only parallel to the bending axis.

For the S2 and S3 series, where the fibres were arranged only parallel (Sx_90 variants) or perpendicular (Sx_0 variants) to the direction of force application, the differences in flexural strength were very large, about 10 times (for the S2 series) and about six times

(for the 3 series) higher flexural stress for Sx_0 variants than for Sx_90.

However, for the S1 and S4 series where the fibres were bi-stacked to the direction of force application, the differences in flexural strength values between Sx_0 and Sx_90 variants were 167 MPa for the S1 series and 239 MPa for the S4 series.

Unidirectional reinforced laminate S2 and S3 series present similar flexural stress vs. displacement characteristics (Figures 3A and 3B)

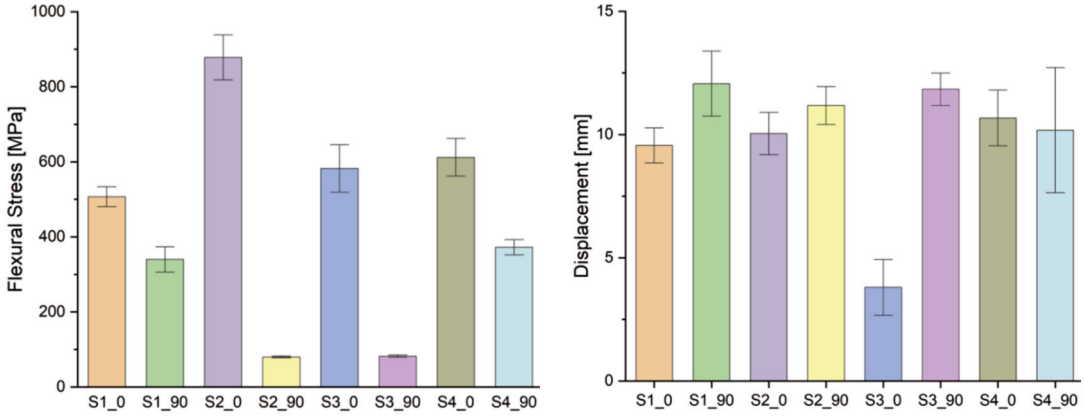

(A) (B)

Figure 4. Results of the static three-point bend test: values of flexural stress (A) and displacement to failure (B).

Significantly, the largest displacements can be observed for specimens mainly reinforced with fibres arranged parallel (Sx_90 variants) to the flexural axis (Figure 4B). In those fibre orientations, the loads in the FRP plies were transferred by the PA6 matrix and can also result in lower flexural stresses for those variants of laminates (Figure 4A). Significantly higher differences in displacement of the variants O and 90 of S3 specimen series than in the other analysed variants of FMLs can be observed. In this case, the mandrel displacement for the S3_90 variant was three times greater than for S3_0. This may be resulted by the unidirectional laminate configuration of the specimens S3_0 variant, $[0^C/0^G{}_4/Alu]_S$, with all of FRP plies with fibres oriented perpendicular to the bending axis, which fully participated in transfer of the bending loads. By contrast, for S3_90 variants of the laminate, all reinforced fibres in FRP plies were oriented parallel to the bending axis, resulting in maximum flexural bending stresses corresponding to the flexural strength of the PA6 matrix. The bidirectional reinforced S4 series specimens contain the same number of the FRP plies as S3 series, but the ratio of the numbers of the fibres oriented parallel and perpendicular to the bending axis oriented was 2/3, which presents smaller differences in displacement values for the S4_0 and S4_90 variants. In that case, as for the previous series of specimens, the flexural strength measured for S4_0 variant specimens was significantly higher than that for S4_90.

The SEM images of the fracture of S1 and S2 samples are presented in Figure 5. It shows typical damage occurred in tests for all variants and configurations (series) of the specimens. Two types of failures are observed: cohesive and adhesive, which are characteristic for FMLs. Cohesive failure is related to the failure within polymeric layers (Figures 5A–5H); however, adhesive failure is referred to the failure at the metal/polymer

interface (Figures 5C and 5D). As can be seen, unidirectional variants of laminates present higher adhesion GFRP layers to the aluminium alloy core (Figures 5E–5H). For both S1_0 and S1_90 series, matrix cracks can be seen (Figures 5A–5D) across GFRP plies with GF fibres oriented parallel to the bending axis.

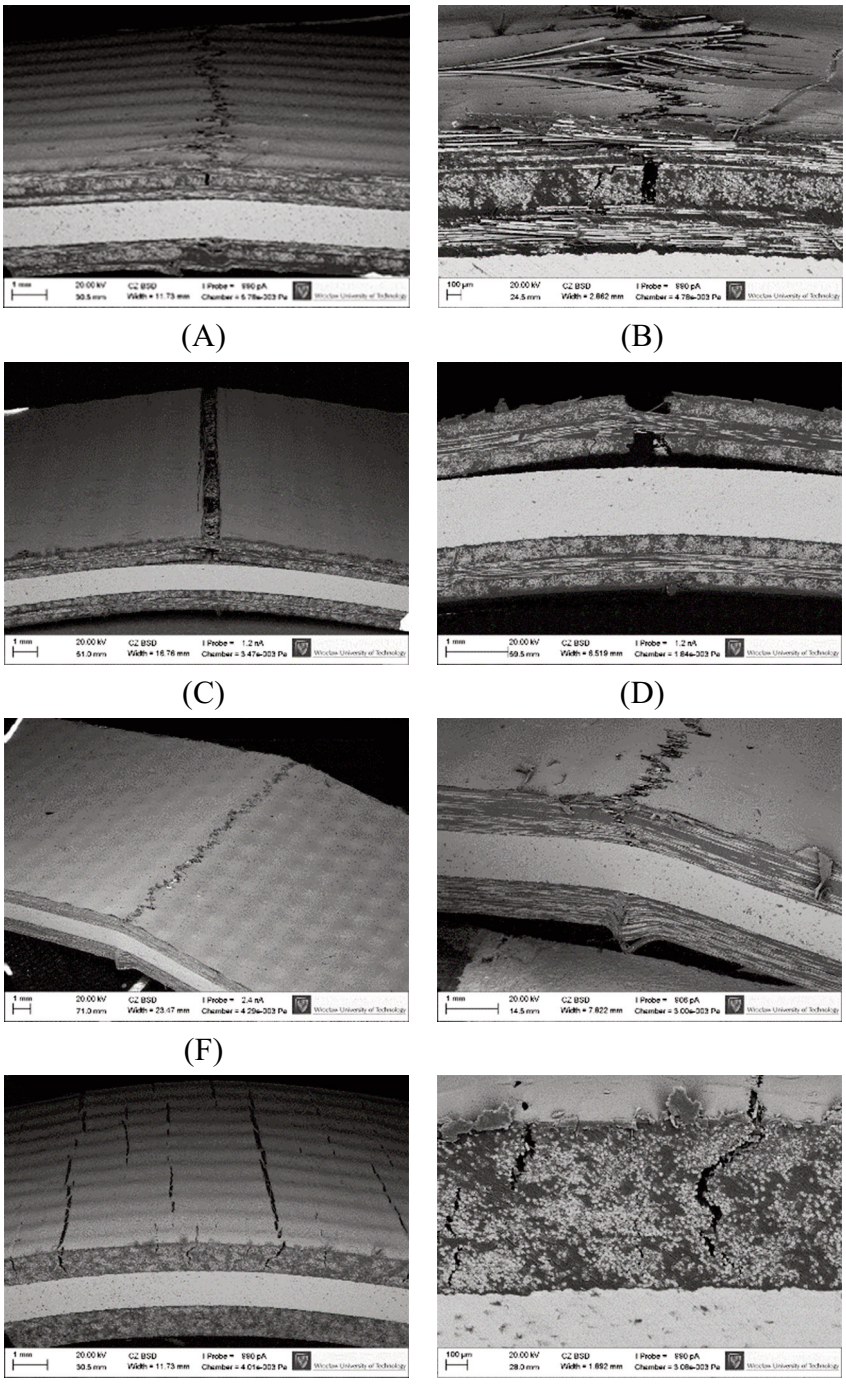

(A) (B)

(C) (D)

(E) (F)

(G) (H)

Figure 5. Views of the damage of specimens caused by the bending test for series: S1_0 (A), (B), S1_90 (C), (D), S2_0 (E), (F), S2_90 (G), (H).

Based on the static three-point bending test, two series S1_0 and S2_0 were selected for fatigue testing. The S1 series was characterised by the smallest difference in flexural strength between the variant when the fibres were arranged only parallel 90^G or perpendicular 0^G to the direction of force application. On the other hand, samples of the S2_0 series are characterised by the largest flexural strength.

The number of applied load cycles was limited to 10^6, and 5 Hz excitation frequency was chosen. For the established frequency, the displacement amplitude of 4 mm was selected. The laminates were considered damaged, and the testing was automatically stopped as soon as one of the two current peak force values fell <80% of the initial comparative value of the very first load cycle.

Tables 3 and 4 show a summary of the specimens used in the three-point bend fatigue test. The table includes information on the values of fatigue flexural stress and number of cycles.

Table 3. Results of the fatigue bend test of the S1_0 series specimen

S1_0						
No.	**Amplitude (mm)**	**Max. fatigue flexural stress (MPa)**	**% of flexural stress**	**Min. fatigue flexural stress (MPa)**	**% of flexural stress**	**Number of cycles**
1	4,04	–245.61	44.69	–35.11	6.39	1,000,000
2	4,04	–346.30	63.01	–99.78	18.16	396,453
3	4,02	–365.06	66.42	–102.85	18.71	335,125
4	4,03	–254.22	46.25	–37.51	6.86	1,000,000
5	4,03	–261.55	47.59	–39.35	7.16	1,000,000
6	4,04	–332.21	60.45	–90.44	16.45	452,144

Table 4. Results of the fatigue bend test of the S2_0 series specimen

S2_0						
No.	**Amplitude (mm)**	**Max. fatigue flexural stress (MPa)**	**% of flexural stress**	**Min. fatigue flexural stress (MPa)**	**% of flexural stress**	**Number of cycles**
1	4,04	–508,63	57.93	–203.81	23.21	183,521
2	4,19	–539,37	61.43	–219.80	25.03	78,751
3	4,04	–549,72	62.61	–220.78	25.14	131,413
4	4,04	–479,31	54.59	–139.82	15.92	1,000,000
5	4,03	–543,90	61.94	–220.66	25.13	132,752
6	4,04	–496,08	56.50	–166.29	18.94	1,000,000

Figure 6 shows the S-N curve for samples of the S_1_0 series. The tests were carried out on six samples from a particular series, and three of six samples reached the limit 10^6 cycles for a flexural stress of approximately 220 MPa (about 43% of static flexural strength). However, for a stress level of 300 MPa, the samples have reached 450,000 cycles.

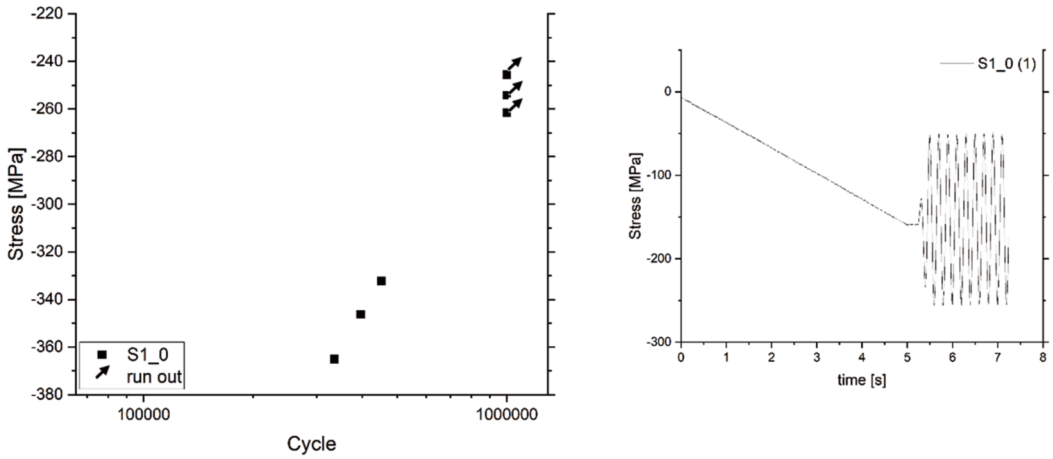

Figure 6. Results of the fatigue test for S1_0 series specimens. (A) S-N curve and (B) flexural stress–time curve.

Figure 7 shows the S-N curve for samples of the S_2_0 series. The tests were carried out on six samples from a particular series, and three of six samples reached the limit 10^6 cycles for a flexural stress of approximately 420 MPa (about 47% of static flexural strength for samples from S_2_0 series). However, for slightly higher stress levels, that is, >450 MPa, the samples run about 183,000 cycles.

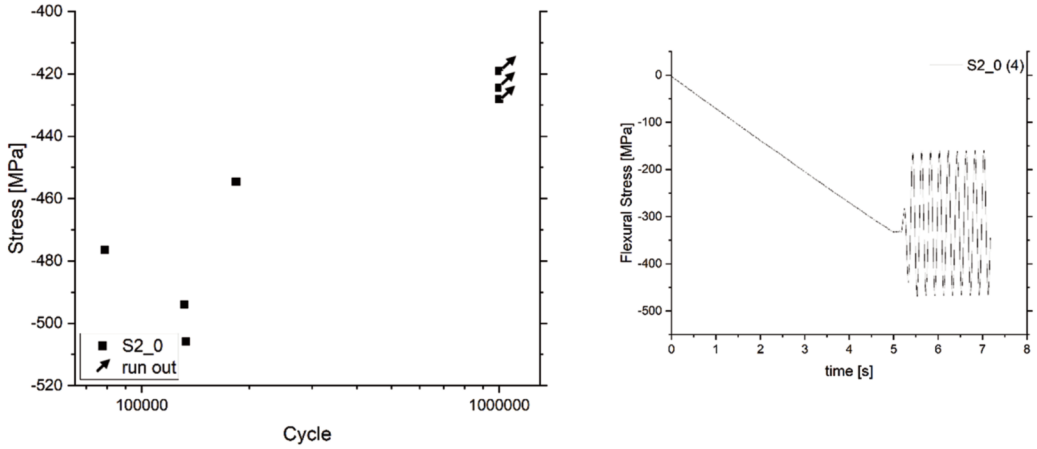

Figure 7. Results of the fatigue test for S2_0 series specimens: (A) S-N curve and (B) flexural stress–time curve.

As presented in Figure 7, the 0 direction specimen of series 2 showed high fatigue load resistance. The crack presented in Figure 8 was caused by a fatigue flexural stress of up to

500 MPa (56% of the measured static bending strength), and the fatigue resistance dropped to 130,000 cycles. It confirmed the high mechanical properties of the proposed inversed hybrid composite configuration.

Figure 8. Views of the fatigue damage of the specimen series 2 occurred after 130,000 cycles.

Discussion

The analysed configurations of S3 series and S4 series FMLs with CFRP layers on the outside of the laminate showed flexural strength similar to the results of the analyses conducted for CARALL laminates obtained by Bellini et al. for the CFRP/al/CFRP ply system (Bellini, Di Cocco, Iacoviello, & Sorrentino, 2019). CARALL specimens made without additional adhesives layers, tested by researchers from the University of Cassino and Southern Lazio, were characterised by a flexural strength of 644–734 MPa, while the measured flexural strength for S3_0 specimens was 582 45 MPa, and that for S4_0 specimens was 611 42 MPa. The CARALL laminates differed from the InverTec FMLs analysed in terms of the number of FRP layers (12 layers), the type of prepreg matrix (epoxy resin), and the alloy type and thickness of the aluminium sheet (AA 1100, 0.6 mm). Available test results indicate a similar range of static flexural strength of FMLs with similar CFRP/aluminium sheet core/CFRP layer configuration.

Table 5. Comparison of the static and fatigue flexural strength of the Invertec, CARALL and CAPPAL FMLs

Type of FML	**InverTec FML**		**CARALL**	**CAPPAL***
	S1_0	**S2_0**	**Case 1 Bellini et al. (2019)**	**Case Zopp et al. (2019)**
Static flexural strength (MPa)	506 ±20	878 ±43	644–734	645 ±16
Fatigue flexural strength (max. number of cycles)	10^6 cycles, up to 7% max flexural stress	10^6 cycles, up to 19% flexural stress	n.d.	10^6 cycles, up to 32% maximum force of bending test

FMLs, fibre metal laminates; n.d., no data.
*CAPPAL – carbon fibre-reinforced polyamide/aluminium laminate (Zopp et al., 2019).

The results of inversed FML bending strength analyses available in the literature indicate that although bending stiffness and bending deformation depend on layers delamination, the use of adhesive layers on the Al core surface decreases flexural strength

of the laminates. The results obtained from the S1 and S2 series samples cannot be related to those of previous work due to the lack of data from the literature related to the analysis of the flexural strength of the inversed FML containing GFRP. The analysed variant of the inversed GLARE (GFRP/Al/GFRP) showed lower flexural strengths with respect to classical GLARE (Bellini et al., 2019), but in this case, the results were affected by significant differences in the FML configuration: the type of the Al alloy used, the number of Al/GFRP layers and the type of matrix (Table 5).

Acknowledgements
The presented studies were performed as part of a CORNET/22/3/2016 project "Load optimized inverse composite technology InverTec" and supported by the National Centre for Research and Development (NCBR) in Poland and Industrial Collective Research (IGF) in Germany and European Research Association for Sheet Metal Working (EFB) to explore integrative in-mould processes with plastic/metal composites. Financial support is gratefully acknowledged.

References

Alderliesten, R. (2017). *Fatigue and fracture of fibre metal laminates*. Cham, Switzerland: Springer International Publishing.

Bellini, C., Di Cocco, V., Iacoviello, F., & Sorrentino, L. (2019). Performance evaluation of CFRP/Al fibre metal laminates with different structural characteristics. *Composite Structures*, *225*, 111117. doi:10.1016/j.compstruct.2019.111117.

Bellini, C., Di Cocco, V., Iacoviello, F., & Sorrentino, L. (2020). Comparison between long and short beam flexure of a carbon fibre based FML. *Procedia Structural Integrity, 26*, 120–128. doi:10.1016/j.prostr.2020.06.015.

Ding, Z., Wang, H., Luo, J., & Li, N. (2021). A review on forming technologies of fibre metal laminates. *International Journal of Lightweight Materials and Manufacture*, *4*, 110–26.

Giasin, K., & Ayvar-Soberanis, S. (2017). Microstructural investigation of drilling induced damage in fibre metal laminates constituents. *Composites Part A: Applied Science and Manufacturing, 97*, 166–78. doi:10.1016/j.compositesa.2017.02.024.

Gunnink, J. W., Vlot, A., Vries, T. J. de., & van der Hoeven, W. (2002). Glare technology development 1997-2000. *Applied Composite Materials, 9*, 201–219.

doi:10.1023/A:1016006314630.

Li, H., Xu, Y., Hua, X., Liu, C., & Tao, J. (2018). Bending failure mechanism and flexural properties of GLARE laminates with different stacking sequences. *Composite Structures, 187*, 354–363. doi:10.1016/j.compstruct.2017.12.068.

Zopp, C., Dittes, A., Nestler, D., Scharf, I., Kroll, L., & Lampke, T. (2019). Quasi-static and fatigue bending behavior of a continuous fiber-reinforced thermoplastic/metal laminate. *Composites Part B: Engineering, 174*, 107043.